

# Low-Complexity and Basis-Free Channel Estimation for Switch-Based mmWave MIMO Systems via Matrix Completion

Rui Hu, Jun Tong, Jiangtao Xi, Qinghua Guo and Yanguang Yu

**Abstract**—Recently, a switch-based hybrid massive MIMO structure that aims to reduce the hardware complexity and power consumption has been proposed as a potential candidate for millimeter wave (mmWave) communications. Exploiting the sparse nature of the mmWave channel, compressive sensing (CS)-based channel estimators have been proposed. When applied to real mmWave channels, the CS-based channel estimators may encounter heavy computational burden due to the high dimensionality of the basis. Meanwhile, knowledge about the response of the antenna array, which is needed for constructing the basis of the CS estimators, may not be perfect due to array uncertainties such as phase mismatch among array elements. This can result in the loss of sparse representation and hence the degraded performance of the CS estimator. In this paper, we propose a novel matrix completion (MC)-based low-complexity channel estimator. The proposed scheme is compatible with switch-based hybrid structures, does not need to specify a basis, and can avoid the basis mismatch issue. Compared with the existing CS-based estimator, the proposed basis-free scheme is immune to array response mismatch and exhibits a significantly lower complexity.

**Index Terms**—Channel estimation, matrix completion, millimeter wave, Massive MIMO.

## I. INTRODUCTION

The enormous amount of spectrum at millimeter wave (mmWave) frequencies (30-300 GHz) and the development in mmWave devices manufacturing technologies make the mmWave communication an attractive candidate for the 5G cellular network [1]. Large-scale multiple-input multiple-output (MIMO) transmission is suggested for mmWave systems to compensate for the significant signal attenuation in the mmWave band. However, a fully digital transceiver structure incurs significant power consumption by the large amount of radio frequency (RF) chains. Phase shifters- or switches-based hybrid structures that employ only a few RF chains have generated considerable interests recently [2], [3].

Employing large-scale MIMO leads to a large channel matrix which needs to be estimated for designing precoders and detectors. Using a conventional channel estimator such as the least squares (LS) estimator demands a large amount of training resources. Fortunately, the mmWave channel matrix tends to be low-rank due to the poor scattering nature at mmWave frequencies [1], [4]. This sparse nature can be exploited to reduce the training data requirement. Compressive sensing (CS)-estimators have recently been proposed for phase shifter- [5] and switch-based [3] mmWave systems, which can reduce the required training time. The CS-based estimators generally need first define and quantize a searching basis, and have good performance with the assumption that the antenna array in the system is ideal, i.e., the predefined basis in the CS-based method is perfectly matched with the actual physical model of the channel. However, in practice, there often exist uncertainties regarding the array response, e.g., due to gain and phase mismatch, mutual coupling and position errors [6]-[11]. With such array uncertainties, it is challenging to construct a proper basis upon which the channel is sparse. Since the performance of a CS-based estimator is sensitive to the choice of the basis [12], [13], a mismatched basis can result in significant performance degradation. Furthermore, the CS methods

The authors are with the School of Electrical, Computer and Telecommunications Engineering, University of Wollongong, Wollongong, NSW 2522, Australia. Email: rh546@uowmail.edu.au, {jtong, jiangtao, qguo, yan-guang}@uow.edu.au.

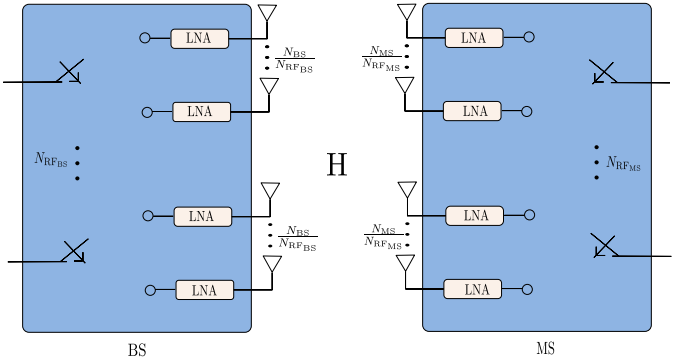


Fig. 1. Switch-based transmitter and receiver structure following the A6 structure of [3]

such as orthogonal matching pursuit (OMP) [3] may suffer from heavy computational load when fine grids are applied to achieve good performance.

In this paper, we study the channel estimation problem for single user switch-based mmWave systems [3] and show the sensitivity of the existing OMP estimator [3] to the phase mismatch of the array. We also propose a basis-free matrix completion (MC)-based channel estimation scheme and show that the mmWave channel satisfies the incoherence properties that enable accurate recovery of the full channel matrix from only a subset of its entries that are sampled uniformly randomly [14]. We then discuss a training scheme that involves only properly controlling the switches at the transmitter and the receiver, which is compatible with the targeted hybrid structure. This scheme guarantees a high probability that at least one sample from each column and each row of the channel matrix is obtained. The singular-value projection (SVP) algorithm [15] is applied to implementing the MC-based estimator and its complexity and parameter choice are analyzed. The simulation results show that the MC scheme, which does not need to specify a basis, has lower complexity than the existing CS-based scheme [3] and is immune to the phase mismatch of the array.

The paper is organized as follows. We introduce the switch-based hybrid mmWave system and review a CS-based channel estimator in Section II. In Section III, we present the proposed MC-based channel estimator. We show the simulation results in Section IV and conclude the paper in Section V.

## II. SYSTEM MODEL

We consider a single user downlink mmWave MIMO system which is the same as in [3]. The system employs the array-subarray hybrid structure (A6) of [3] at both the base station (BS) and mobile station (MS): At the BS, each of the  $N_{BS}$  transmit antennas is equipped with a switch, and every  $N_{BS}/N_{RF_{BS}}$  neighbouring switches are grouped together and connected to one of the  $N_{RF_{BS}}$  RF chains. The MS has the same structure, with  $N_{MS}$  antennas and  $N_{RF_{MS}}$  RF chains. The diagram of this structure is shown in Fig. 1. Following [5], the  $N_{MS} \times N_{BS}$  downlink mmWave channel matrix is given by

$$\mathbf{H} = \mathbf{A}_{MS} \text{diag}(\boldsymbol{\alpha}) \mathbf{A}_{BS}^H, \quad (1)$$

where  $\mathbf{A}_{BS} = [\mathbf{a}_{BS}(\phi_1), \mathbf{a}_{BS}(\phi_2), \dots, \mathbf{a}_{BS}(\phi_L)]$ ,  $(\cdot)^H$  denotes conjugate transpose,  $\mathbf{a}_{BS}(\phi_l)$  is a steering vector of the angle of departure (AoD)  $\phi_l$  of the  $l$ -th path, and  $L$  is the number of paths. Similarly, we can define  $\mathbf{A}_{MS} = [\mathbf{a}_{MS}(\theta_1), \mathbf{a}_{MS}(\theta_2), \dots, \mathbf{a}_{MS}(\theta_L)]$ , where  $\mathbf{a}_{MS}(\theta_l)$  is the steering vector of the angle of arrival (AoA)  $\theta_l$ . Assuming ideal uniform linear arrays (ULA) with distance  $d$  between adjacent antennas and there are no amplitude, phase or

antenna positioning errors, the steering vector is given by

$$\mathbf{a}_{\text{BS}}(\phi_l) = \frac{1}{\sqrt{N_{\text{BS}}}} [1, e^{j\frac{2\pi}{\lambda}d \sin(\phi_l)}, \dots, e^{j(N_{\text{BS}}-1)\frac{2\pi}{\lambda}d \sin(\phi_l)}]^T, \quad (2)$$

where  $\lambda$  is the wavelength. The steering vector  $\mathbf{a}_{\text{MS}}(\theta_l)$  is defined similarly. The path gains are modeled as

$$\boldsymbol{\alpha} = \sqrt{\frac{N_{\text{BS}}N_{\text{MS}}}{L}} [\alpha_1, \alpha_2, \dots, \alpha_L]^T,$$

where  $\alpha_l$  is the complex gain of the  $l$ -th path, which is assumed to be i.i.d.  $\mathcal{CN}(0, \sigma_\alpha^2)$  distributed.

The OMP can be applied to estimating the above  $\mathbf{H}$  [2]-[5], especially for channels with a small number  $L$  of paths. Ignoring the quantization error, using the virtual channel representation  $\mathbf{H}$  may be modeled as [3], [16], [17],

$$\mathbf{H} = \mathbf{A}_{\text{MSD}} \mathbf{H}_v \mathbf{A}_{\text{BSD}}^H, \quad (3)$$

where  $\mathbf{A}_{\text{MSD}} \in \mathbb{C}^{N_{\text{MS}} \times G_r}$  and  $\mathbf{A}_{\text{BSD}} \in \mathbb{C}^{N_{\text{BS}} \times G_t}$  are two dictionary matrices, and  $\mathbf{H}_v \in \mathbb{C}^{G_r \times G_t}$  is a sparse matrix that contains the path gains of the quantized directions. The two dictionary matrices  $\mathbf{A}_{\text{MSD}}$  and  $\mathbf{A}_{\text{BSD}}$  are commonly constructed using steering vectors [3], [5]. Vectorizing (3) leads to

$$\text{vec}(\mathbf{H}) = \boldsymbol{\Psi} \mathbf{x}, \quad (4)$$

where

$$\boldsymbol{\Psi} = \mathbf{A}_{\text{BSD}}^* \otimes \mathbf{A}_{\text{MSD}} \quad (5)$$

is the basis matrix,  $(\cdot)^*$  denotes conjugate,  $\otimes$  represents Kronecker product, and  $\mathbf{x} \triangleq \text{vec}(\mathbf{H}_v)$  is an  $L$ -sparse vector. Noisy observations of linear combinations of the entries of  $\text{vec}(\mathbf{H})$  may be obtained by training, yielding

$$\mathbf{y} = \boldsymbol{\Phi} \text{vec}(\mathbf{H}) + \mathbf{z} = \boldsymbol{\Phi} \boldsymbol{\Psi} \mathbf{x} + \mathbf{z}, \quad (6)$$

where  $\boldsymbol{\Phi}$  is the sensing matrix specified by the training scheme and  $\mathbf{z}$  is the noise. The OMP method finds the non-zero entries of  $\mathbf{x}$  from  $\mathbf{y}$ , which corresponds to finding  $L$  out of  $G_r G_t$  candidate direction pairs. In order to obtain the row orthogonality of the two dictionaries, the physical angles of the steering vector should be generated according to the following equation [18]

$$\frac{2\pi d}{\lambda} \sin(\theta_g) = \frac{2\pi}{G} (g-1) - \pi, \quad g = 1, 2, \dots, G, \quad (7)$$

where  $G$  is the number of grid points,  $d$  is the distance between two neighbouring elements, and  $\lambda$  is the wavelength. If  $d = \frac{\lambda}{2}$ , equation (7) simplifies to

$$\sin(\theta_g) = \frac{2}{G} (g-1) - 1. \quad (8)$$

Under this condition, when the numbers of grid points  $G_t = N_{\text{BS}}$ ,  $G_r = N_{\text{MS}}$ , the two dictionary matrices  $\mathbf{A}_{\text{MSD}}$  and  $\mathbf{A}_{\text{BSD}}$  are unitary. When  $G_t > N_{\text{BS}}$  and  $G_r > N_{\text{MS}}$ , the two dictionary matrices are redundant. The computational complexity of the OMP method is about  $8N G_t G_r$  flops per iteration. In general, the larger the numbers of grid points the better the performance, yet the heavier the computational burden.

The above analysis of CS-based estimator is under the assumption that the channel has a sparse representation under the ideal steering vector basis. When uncertainties about the array response are presented as mentioned in Section I, the actual channel may not be sparse on the basis defined in (5). Denote the unknown phase error

at antenna element  $i$  as  $\gamma_i$ . The real steering vector is

$$\mathbf{a}_{\text{BS,real}}(\phi_l) = \frac{1}{\sqrt{N_{\text{BS}}}} [e^{j\gamma_1}, e^{j(\frac{2\pi}{\lambda}d \sin(\phi_l) + \gamma_2)}, \dots, e^{j(\frac{2\pi}{\lambda}(N_{\text{BS}}-1)d \sin(\phi_l) + \gamma_{N_{\text{BS}}})}]^T, \quad (9)$$

which depends not only on the AoA and AoD, but also on the phase error. In this paper, we will demonstrate the performance degradation of the OMP estimator due to phase mismatch through simulations in Section IV. Even the unknown phase mismatch can cause the basis mismatch issue [13] on CS-based methods, the channel matrix  $\mathbf{H}$  itself remains to be low-rank whenever the number of paths  $L$  is small. In Section III, we introduce a MC approach which is basis-free and is thus immune to the uncertainties of array response.

### III. MATRIX COMPLETION FOR MMWAVE CHANNEL ESTIMATION

The MC problem is to recover an unknown low-rank matrix  $\mathbf{M}$  from a subset of entries sampled through the operator  $P_\Omega(\cdot)$  defined by

$$[P_\Omega(\mathbf{X})]_{i,j} = \begin{cases} [\mathbf{X}]_{i,j}, & (i,j) \in \Omega \\ 0, & \text{otherwise} \end{cases}, \quad (10)$$

where  $[\mathbf{X}]_{i,j}$  denotes the  $(i,j)$ -th entry of  $\mathbf{X}$ . The number of sampled entries of  $\mathbf{X}$  in the operator  $P_\Omega(\cdot)$  is  $pN$ , where  $p$  is the sampling density and  $N$  is the total number of entries in  $\mathbf{X}$ . The recovery task is to solve

$$\min_{\mathbf{X}} \text{rank}(\mathbf{X}), \quad \text{s.t.} \quad P_\Omega(\mathbf{X}) = P_\Omega(\mathbf{M}). \quad (11)$$

This problem is NP-hard and usually solved approximately, e.g., as a nuclear norm minimization problem [19] or an affine rank minimization problem (ARMP) [15]. In this section, following the similar steps in [20], we first show the suitability of MC for mmWave channel estimation by examining the incoherence property of the mmWave MIMO channel. We then introduce a training scheme that is compatible with the switch-based structure and discuss the estimation algorithm and its complexity.

#### A. Incoherence Property of mmWave Channel

We assume large  $N_{\text{MS}}$  and  $N_{\text{BS}}$ , which is of interest for mmWave applications. We first check the incoherence property of the mmWave channel with ideal antenna arrays. Let the singular value decomposition (SVD) of the rank- $L$  matrix  $\mathbf{H}$  be

$$\mathbf{H} = \sum_{k=1}^L \sigma_k \mathbf{u}_k \mathbf{v}_k^H, \quad (12)$$

where  $\sigma_k$  denotes the  $k$ -th singular value and  $\mathbf{u}_k$  and  $\mathbf{v}_k$  are the corresponding left and right singular vectors, respectively. Define

$$\mathbf{P}_U = \sum_{i=1}^L \mathbf{u}_i \mathbf{u}_i^H, \quad \mathbf{P}_V = \sum_{i=1}^L \mathbf{v}_i \mathbf{v}_i^H, \quad \mathbf{E} = \sum_{i=1}^L \mathbf{u}_i \mathbf{v}_i^H. \quad (13)$$

Let  $\mathbf{e}_a$  denote the vector with the  $a$ -th entry equal to 1 and others equal to zero,  $1_{a=a'} = 1$  if  $a = a'$  is true and  $1_{a=a'} = 0$  otherwise. If there exists  $\mu$  such that

- for all pairs  $(a, a')$  and  $(b, b')$

$$\left| \langle \mathbf{e}_a, \mathbf{P}_U \mathbf{e}_{a'} \rangle - \frac{L}{N_{\text{MS}}} 1_{a=a'} \right| \leq \mu \frac{\sqrt{L}}{N_{\text{MS}}} \quad (14)$$

$$\left| \langle \mathbf{e}_b, \mathbf{P}_V \mathbf{e}_{b'} \rangle - \frac{L}{N_{\text{BS}}} 1_{b=b'} \right| \leq \mu \frac{\sqrt{L}}{N_{\text{BS}}}, \quad (15)$$

- and for all  $(a, b)$ ,

$$|\mathbf{E}_{ab}| \leq \mu \frac{\sqrt{L}}{\sqrt{N_{\text{MS}} N_{\text{BS}}}}, \quad (16)$$

then  $\mathbf{H}$  obeys the strong incoherence property with parameter  $\mu$  [21]. In this case,  $\mathbf{H}$  can be recovered without error with high probability if at least  $C_1 \mu^4 n (\log n)^2$  uniformly sampled entries are known [21], where  $C_1$  is a constant and  $n = \max(N_{\text{MS}}, N_{\text{BS}})$ .

We start examining the incoherence property of  $\mathbf{H}$  from  $L = 1$ . When  $L = 1$ , comparing (1) with (12), we can see that  $\mathbf{u}_1 = \mathbf{a}_{\text{MS}}(\theta_1)$  and  $\mathbf{v}_1 = \mathbf{a}_{\text{BS}}(\phi_1)$  are the singular vectors, all entries of  $\mathbf{P}_U$  have the same module  $1/N_{\text{MS}}$ . When  $a = a'$ ,

$$\langle \mathbf{e}_a, \mathbf{P}_U \mathbf{e}_{a'} \rangle = [\mathbf{P}_U]_{a,a} = \frac{1}{N_{\text{MS}}},$$

which yields  $|\langle \mathbf{e}_a, \mathbf{P}_U \mathbf{e}_{a'} \rangle - \frac{1}{N_{\text{MS}}} \mathbf{1}_{a=a'}| = 0$ . When  $a \neq a'$ ,

$$|\langle \mathbf{e}_a, \mathbf{P}_U \mathbf{e}_{a'} \rangle| = |[\mathbf{P}_U]_{a,a'}| = \frac{1}{N_{\text{MS}}}.$$

We can now verify that (14) is satisfied with  $\mu = 1$ . Similarly, we can verify (15) and (16) with  $\mu = 1$ .

For  $L \geq 2$ , we exploit the following asymptotic property of mmWave channel [22]: As  $N_{\text{MS}}$  and  $N_{\text{BS}}$  become very large, the singular vectors of  $\mathbf{H}$  converge to the steering vectors. Assume  $\mathbf{u}_i = \mathbf{a}_{\text{MS}}(\theta_i)$ ,  $\mathbf{v}_i = \mathbf{a}_{\text{BS}}(\phi_i)$ , then all the entries of the left singular vectors have module  $1/\sqrt{N_{\text{MS}}}$  and those of the right singular vectors have module  $1/\sqrt{N_{\text{BS}}}$ . Consequently, for  $a = a'$ ,

$$\langle \mathbf{e}_a, \mathbf{P}_U \mathbf{e}_{a'} \rangle = [\mathbf{P}_U]_{a,a} = \frac{L}{N_{\text{MS}}}, \quad (17)$$

and for  $a \neq a'$ ,

$$\begin{aligned} |\langle \mathbf{e}_a, \mathbf{P}_U \mathbf{e}_{a'} \rangle| &= |[\mathbf{P}_U]_{a,a'}| = \left| \sum_{i=1}^L u_{i,a} u_{i,a'}^* \right| \\ &\leq \sum_{i=1}^L |u_{i,a}| |u_{i,a'}^*| = \frac{L}{N_{\text{MS}}} \end{aligned} \quad (18)$$

From (17) and (18) we can verify that (14) is satisfied with  $\mu = \sqrt{L}$ . Similarly we can verify (15) and (16).

Based on the above analysis, the mmWave channel  $\mathbf{H}$  without phase mismatches obeys the strong incoherence property with parameter  $\mu \approx \sqrt{L}$  when  $\mathbf{H}$  is large and thus can be recovered from a subset of its entries according to the MC theory.

When phase mismatches are present, it can be seen from (9) that compared to the ideal steering vector, the amplitude of each element in the real steering vector  $\mathbf{a}_{\text{BS,real}}(\phi_i)$  does not change. Hence the analysis for the channel under ideal antenna array assumption can still stand with the channel that has phase mismatch. The above analysis assumes noiseless samples of  $\mathbf{H}$  and provides useful guidelines for high-SNR applications.

## B. Training Scheme

The sampling pattern has a crucial influence on the performance of MC. From [21], at least one entry must be sampled from each row and each column to recover the original matrix. In this paper, we adapt the uniform spatial sampling (USS) scheme [20], which was proposed for array signal processing and seems to outperform alternative sampling schemes such as the Bernoulli scheme [21, Section IV].

Suppose  $M$  entries of the  $N_{\text{MS}} \times N_{\text{BS}}$  matrix  $\mathbf{H}$  need to be sampled. The USS scheme suggests to take  $M/N_{\text{BS}}$  distinct samples from the  $N_{\text{MS}}$  entries of each column. In our switch-based array-subarray structure, there are  $N_{\text{sub}} \triangleq N_{\text{MS}}/N_{\text{RF,MS}}$  antennas in each MS subarray which share the same RF chain. In order to make full use

of the MS RF chains and keep the training time short, all the  $N_{\text{RF,MS}}$  MS RF chains are activated during the whole training process. Each MS RF chain is switched randomly to a distinct antenna in the associated subarray and  $N_{\text{RF,MS}}$  samples can be produced at each training stage. Thus, in total  $N_s = M/N_{\text{RF,MS}}$  training stages are used.

We now describe the training process. We index the BS antennas from 1 to  $N_{\text{BS}}$  and MS antennas from 1 to  $N_{\text{MS}}$ . Let  $\mathbf{Y} \in \mathbb{C}^{N_{\text{MS}} \times N_{\text{BS}}}$  and initialize all its entries to zero. For each MS subarray  $k$ ,  $k = 1, 2, \dots, N_{\text{RF,MS}}$ , denote by  $\mathcal{I}_k$  the set of the antennas that have not been switched on so far. The disjoint sets  $\{\mathcal{I}_k\}$  are initialized according to the array structure and the union of the initial  $\mathcal{I}_k$  gives  $\{1, 2, \dots, N_{\text{MS}}\}$ . At the  $t$ -th training stage,

- At the BS, only the transmit antenna indexed by  $j_t \equiv \text{mod}(t, N_s)$  is switched on and a known symbol  $s$  is sent. For each MS subarray  $k$ , randomly switch on (with equal probabilities) an antenna in  $\mathcal{I}_k$  and denote by  $i_k$  the index of the antenna switched on. The received symbol at the  $i_k$ -th MS antenna is written as

$$r_{i_k} = [\mathbf{H}]_{i_k, j_t} s + n_{i_k}, \quad k = 1, 2, \dots, N_{\text{RF,MS}}. \quad (19)$$

- For  $k = 1, 2, \dots, N_{\text{RF,MS}}$ ,

$$[\mathbf{Y}]_{i_k, j_t} = \frac{r_{i_k}}{s},$$

and remove  $i_k$  from  $\mathcal{I}_k$ .

The above simple training process yields noisy observations of  $M$  distinct entries of  $\mathbf{H}$ , which are recorded in  $\mathbf{Y}$ . When  $N_s \geq N_{\text{BS}}$ , i.e.,  $M \geq N_{\text{BS}} N_{\text{RF,MS}}$ , it is guaranteed that at least one entry is observed (with noise) for each column of  $\mathbf{H}$  as every BS antenna is switched on at least once. The sampling scheme also guarantees that for each MS subarray,  $M/(N_{\text{BS}} N_{\text{RF,MS}})$  out of the  $N_{\text{sub}}$  entries of each column of  $\mathbf{H}$  have been sampled once. The event of missing an entire row of  $\mathbf{H}$  corresponds to the case that for all the  $N_{\text{BS}}$  columns, the  $M/(N_{\text{BS}} N_{\text{RF,MS}})$  entries are taken from a common subset of the subarray with size  $N_{\text{sub}} - 1$ . The probability of such an event is

$$P_{\text{miss}} = \left( \frac{\left( \frac{N_{\text{sub}} - 1}{\frac{M}{N_{\text{BS}} N_{\text{RF,MS}}}} \right)}{\left( \frac{N_{\text{sub}}}{\frac{M}{N_{\text{BS}} N_{\text{RF,MS}}}} \right)} \right)^{N_{\text{BS}}} = \left( \frac{N_{\text{MS}} - \frac{M}{N_{\text{BS}}}}{N_{\text{MS}}} \right)^{N_{\text{BS}}}, \quad (20)$$

which is negligible when  $M$  and  $N_{\text{BS}}$  are large enough. For example, when  $N_{\text{MS}} = 16$ ,  $N_{\text{BS}} = 64$ , and  $M = 0.5 \times N_{\text{MS}} N_{\text{BS}}$ ,  $P_{\text{miss}} \approx 5.4 \times 10^{-20}$ .

## C. Singular Value Projection (SVP)

After the training process, we apply singular value projection (SVP) algorithm [15] to reconstruct  $\mathbf{H}$ . The algorithm is to solve the following matrix sensing problem

$$\min_{\mathbf{X}} \psi(\mathbf{X}) = \frac{1}{2} \|\mathcal{A}(\mathbf{X}) - \mathbf{b}\|_F^2, \text{ s.t. rank}(\mathbf{X}) \leq L, \quad (21)$$

where  $\mathcal{A}$  is a linear map,  $\mathbf{b}$  is the observed signal and  $L$  is the maximum rank of the matrix  $\mathbf{X}$ . The MC problem is a special case of the above matrix sensing problem, which replaces the sensing operator  $\mathcal{A}$  by the operator  $P_\Omega$  defined in (10). Therefore the problem becomes

$$\min_{\mathbf{X}} \psi(\mathbf{X}) = \frac{1}{2} \|P_\Omega(\mathbf{X}) - P_\Omega(\mathbf{Y})\|_F^2, \text{ s.t. rank}(\mathbf{X}) \leq L, \quad (22)$$

where  $\Omega$  characterizes the sampling pattern. A similar algorithm has been applied to MIMO channel estimation in a different scenario in

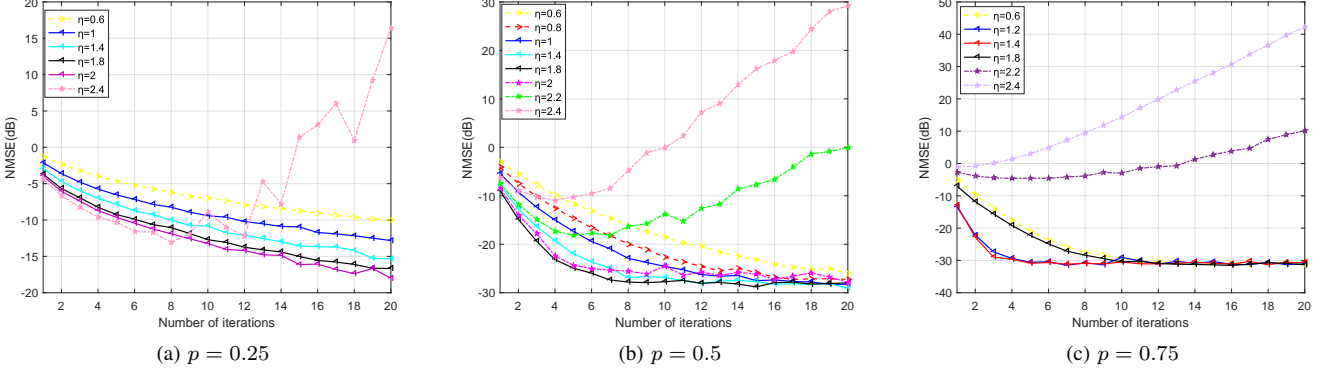


Fig. 2. Convergence performance with different levels of  $\eta$  and  $p$  for the system where  $N_{BS} = N_{MS} = 64$ ,  $L = 4$ , SNR= 25 dB.

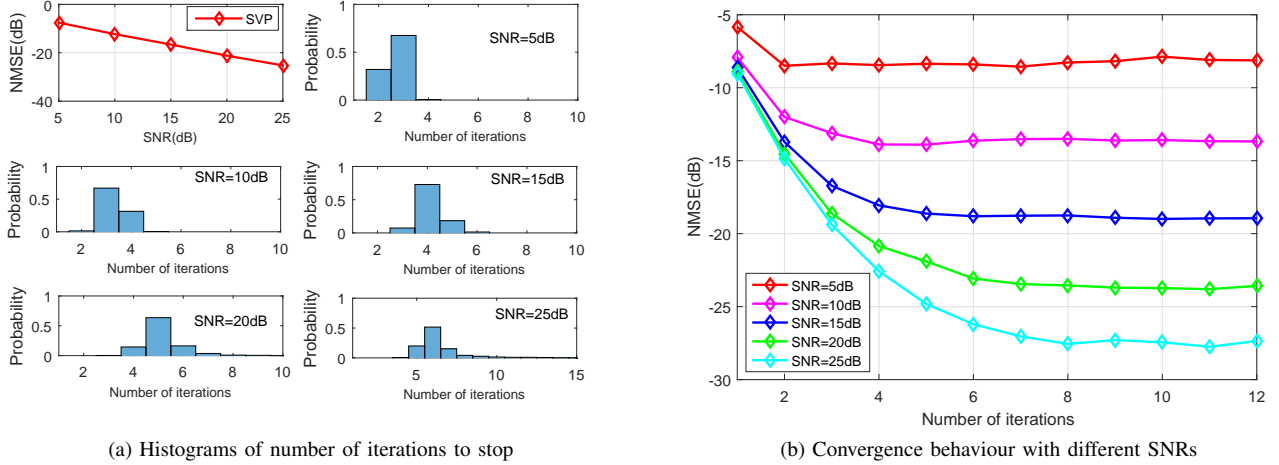


Fig. 3. Stopping performance using the tolerance  $\epsilon$  for the system where  $N_{BS} = N_{MS} = 64$ ,  $L = 4$ ,  $p = 0.5$ ,  $\eta = 1.8$ .

#### Algorithm 1 Singular Value Projection (SVP)

**Input:**  $P_\Omega(\mathbf{Y})$ ,  $L$ ,  $\eta$ ,  $\epsilon$

**Initialization:**  $\mathbf{X}^0 = \mathbf{0}$ ,  $t = 0$

1. **repeat**

2.  $\mathbf{Z}^{t+1} \leftarrow \mathbf{X}^t - \eta(P_\Omega(\mathbf{X}^t) - P_\Omega(\mathbf{Y}))$

3. Compute the top  $L$  singular vectors of  $\mathbf{Z}^{t+1}$ :  $\mathbf{U}_L$ ,  $\Sigma_L$ ,  $\mathbf{V}_L$

4.  $\mathbf{X}^{t+1} \leftarrow \mathbf{U}_L \Sigma_L \mathbf{V}_L^H$

5.  $t = t + 1$

6. Until  $\|P_\Omega(\mathbf{X}^t) - P_\Omega(\mathbf{Y})\|_2^2 \leq \epsilon$

**Output** the channel estimate  $\widehat{\mathbf{H}} = \mathbf{X}^t$

[23]. The SVP algorithm for solving the MC problem is shown in Algorithm I. The major computational cost of the SVP is in Step 4, which needs to compute the rank- $L$  approximation of a  $N_{MS} \times N_{BS}$  intermediate matrix  $\mathbf{Z}$ . This can be done by computing the SVD of  $\mathbf{Z}$ . In order to reduce the high computational complexity due to SVD, we can choose an alternative way to calculate the rank- $L$  approximation of  $\mathbf{Z}$  by first computing the eigenvalue decomposition of the  $N_{MS} \times N_{MS}$  matrix  $\mathbf{Z}\mathbf{Z}^H = \mathbf{U}\mathbf{S}\mathbf{U}^H$ , and then obtaining  $\mathbf{Z}_L = \mathbf{U}_L \mathbf{U}_L^H \mathbf{Z}$ , where  $\mathbf{U}_L$  consists of columns in  $\mathbf{U}$  that correspond to the  $L$  largest eigenvalues. This way the computational cost of the SVP algorithm is about  $16N_{MS}^2 N_{BS} + 23N_{MS}^3 + 8N_{MS}^2 L$  flops per iteration.

The convergence of the iterative SVP algorithm is influenced by the step size  $\eta$ . A small step size guarantees convergence but has low convergence rate, while a large step size implies fast convergence yet has the risk of divergence. The authors of [15] analyzed the convergence condition of the SVP algorithm for solving the general

matrix sensing problem in (21) and suggested to set the step size  $\eta < 1$  in order to obtain the convergence of the SVP. For the MC problem of this paper, a special case of the matrix sensing problem, setting  $\eta < 1$  guarantees the convergence of the SVP. However, our analysis in the Appendix suggests that it is possible to set  $\eta > 1$  for faster convergence of the SVP. The simulation results in Fig. 2 support our analysis and indicate that setting  $1 < \eta < 2$  for the SVP has faster convergence than setting  $\eta < 1$ . Furthermore, the results also suggest that setting  $\eta > 2$  for the SVP when solving the MC problem has a risk of diverging.

#### IV. SIMULATION RESULTS

We first show the influence of  $\eta$  on the convergence rate of the SVP estimator. We assume that there are  $N_{BS} = 64$  BS antennas and  $N_{MS} = 64$  MS antennas, and there are  $N_{RF_{MS}} = N_{RF_{BS}} = 16$  RF chains at the MS and the BS, respectively. The number of paths, i.e., the rank of the channel matrix, is  $L = 4$ . The signal-to-noise ratio (SNR) is 25dB. The AoAs and AoDs of  $\mathbf{H}$  are uniformly distributed in  $[-\pi/2, \pi/2]$ , and  $\sigma_\alpha^2$  is set to 1. We use the normalized mean squared error (NMSE) defined as  $\|\mathbf{H} - \widehat{\mathbf{H}}\|_F^2 / \|\mathbf{H}\|_F^2$  to evaluate the performance of SVP. Under this system setting and using our proposed sampling scheme, Fig. 2 (a)-(c) show the convergence behaviour for different  $\eta$  with sampling density  $p = 0.25, 0.5, 0.75$ , respectively. It can be seen from Fig. 2 that when  $\eta < 2$ , the SVP converges for all the three cases, and faster convergence occurred when  $\eta > 1$  rather than  $\eta < 1$ . For sampling density  $p = 0.25$ ,

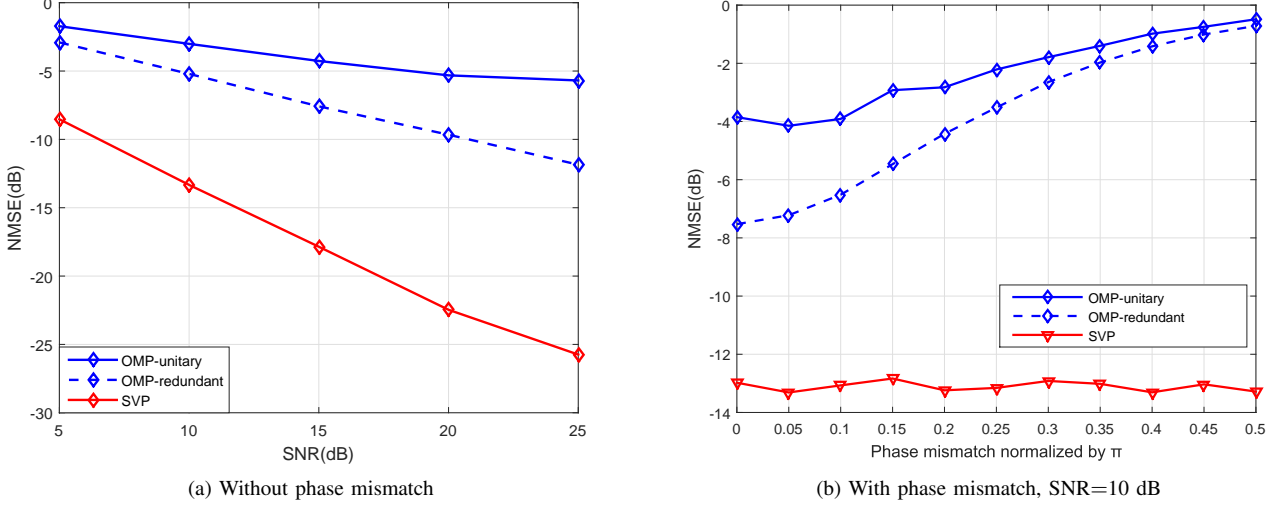


Fig. 4. Comparison between OMP estimator and SVP estimator without and with phase mismatch for the system where  $N_{\text{BS}} = N_{\text{MS}} = 64, L = 4, p = 0.5, \eta = 1.8$ .

when  $\eta = 2.4$  the SVP diverged, and for  $p = 0.5$  and  $p = 0.75$ , the SVP diverges when  $\eta > 2$ . The simulation results show that setting the step size  $\eta$  in between 1 and 2 results in convergence and achieves faster convergence rate than setting  $\eta < 1$ .

Based on the convergence analysis in [15], the tolerance  $\epsilon$  of Algorithm I can be set as  $\epsilon = C\|\mathbf{e}\|_F^2 + \epsilon_0$ , where  $\|\mathbf{e}\|_F^2$  is the instantaneous total noise power of the observed entries,  $C$  and  $\epsilon_0$  are constants. Since  $\|\mathbf{e}\|_F^2$  is unknown, we use  $pN_{\text{BS}}N_{\text{MS}}\sigma^2$  to approximate  $C\|\mathbf{e}\|_F^2$ , where  $\sigma^2$  is the average noise power. Fig 3 (a) shows the stopping performance of using this tolerance  $\epsilon$  for a system with  $N_{\text{BS}} = N_{\text{MS}} = 64, L = 4, p = 0.5, \eta = 1.8$ , and  $\epsilon_0 = 10^{-3}$ . As shown in the histogram in Fig. 3 (a), the convergence rate is different for different SNRs. For SNR = 5, 10, 15, 20, 25 dB, it takes 3, 3, 4, 5, 6 iterations on average for the SVP to stop respectively, which are consistent with the results in Fig. 3 (b). The simulation results in Fig. 3 suggest the tolerance can stop the algorithm properly.

We next show the estimation performance and the computational complexity comparison between the OMP estimator discussed in Section II and the proposed SVP estimator. Suppose we have  $N_{\text{BS}} = N_{\text{MS}} = 64, N_{\text{RF}_{\text{MS}}} = N_{\text{RF}_{\text{BS}}} = 16, L = 4, p = 0.5$ . For the OMP, two dictionaries are adopted, one is unitary with  $G_t = 64, G_r = 64$  grid points and the other is redundant with  $G_t = 128, G_r = 128$  grid points. For the SVP, we set the step size  $\eta = 1.8$ . For the unitary basis, the per-iteration complexity ratio between the OMP estimator and the SVP estimator is around  $8pN_{\text{BS}}N_{\text{MS}}G_tG_r/(16N_{\text{MS}}^2N_{\text{BS}} + 23N_{\text{MS}}^3 + 8N_{\text{MS}}^2L) \approx 6.5$ , and for the redundant basis, the ratio increases to 26. We aim to compare the estimation performance of the OMP and SVP while considering their computational complexity. As both the OMP and SVP algorithms are iterative, we set the number of iterations of the OMP and the SVP to be the same in order to compare their computational complexity. Under different levels of SNR, we set the number of the iterations differently, which is 2 for SNR = 5 dB, 3 for SNR = 10 dB, 4 for SNR = 15 dB, 5 for SNR = 20 dB and 6 for SNR = 25 dB. This setting is based on the observation in Fig. 3. Hence the total computational complexity for the OMP-unitary is 6.5 times that of the SVP, and for the OMP-redundant is 26 times that of the SVP. The comparison result in Fig. 4(a) shows that under this system setting, the SVP estimator can achieve better performance than the OMP estimator while has much lower computational complexity.

As mentioned in Section II, there can be phase mismatch among array elements in the antenna array in practice. The OMP estimator that depends on the basis is sensitive to this array non-ideality. By contrast, the SVP estimator, which is independent of the basis, is immune to the phase mismatch. This is demonstrated in Fig. 4(b). We assumed that the unknown phase error is uniformly distributed as  $\gamma \sim U[-\gamma_{\text{max}}, \gamma_{\text{max}}]$  and simulated 11 different levels of phase mismatch by setting  $\gamma_{\text{max}} = \{0, 0.05\pi, \dots, 0.5\pi\}$ . Fig. 4(b) suggests that the performance of the OMP estimator degrades as the phase mismatch becomes larger but the SVP estimator has stable performance under different levels of phase mismatch.

## V. CONCLUSIONS

In this paper, we show that matrix completion can be used for mmWave channel estimation. An estimation scheme that is compatible with the switch-based hardware structure is proposed. We show that the SVP method can exhibit significantly lower complexity than the OMP scheme and is immune to the phase mismatch of the array.

## VI. APPENDIX

We denote the exact solution of (22) to be  $\mathbf{X}^*$ . Then for the noiseless case we have  $P_{\Omega}(\mathbf{Y}) = P_{\Omega}(\mathbf{X}^*)$ . Hence the objective function  $\psi(\mathbf{X})$  in (22) can be written as

$$\psi(\mathbf{X}) = \frac{1}{2}\|P_{\Omega}(\mathbf{X} - \mathbf{Y})\|_F^2 = \frac{1}{2}\|P_{\Omega}(\mathbf{X} - \mathbf{X}^*)\|_F^2.$$

We also define an operator  $P_{\Omega}^{\perp}$  so that

$$P_{\Omega}^{\perp}(\mathbf{X}) = \mathbf{X} - P_{\Omega}(\mathbf{X}).$$

Note that there are  $pN$  entries sampled from  $\mathbf{X}$  in  $P_{\Omega}(\mathbf{X})$ , where  $N$  is the total number of entries of  $\mathbf{X}$ . Thus there are  $(1-p)N$  entries

from  $\mathbf{X}$  in  $P_\Omega^\perp(\mathbf{X})$ . We then have

$$\begin{aligned}
\sqrt{2\psi(\mathbf{X}^{t+1})} &= \|P_\Omega(\mathbf{X}^{t+1} - \mathbf{X}^*)\|_F \\
&= \|P_\Omega(\mathbf{X}^{t+1} - \mathbf{Z}^{t+1} + \mathbf{Z}^{t+1} - \mathbf{X}^*)\|_F \\
&= \|P_\Omega(\mathbf{X}^{t+1} - \mathbf{Z}^{t+1}) + P_\Omega(\mathbf{Z}^{t+1} - \mathbf{X}^*)\|_F \\
&\stackrel{(a)}{\leq} \|P_\Omega(\mathbf{X}^{t+1} - \mathbf{Z}^{t+1})\|_F + \|P_\Omega(\mathbf{Z}^{t+1} - \mathbf{X}^*)\|_F \\
&\stackrel{(b)}{\leq} \|\mathbf{X}^{t+1} - \mathbf{Z}^{t+1}\|_F + \|P_\Omega(\mathbf{Z}^{t+1} - \mathbf{X}^*)\|_F \\
&\stackrel{(c)}{\leq} \|\mathbf{Z}^{t+1} - \mathbf{X}^*\|_F + \|P_\Omega(\mathbf{Z}^{t+1} - \mathbf{X}^*)\|_F \\
&= \|P_\Omega^\perp(\mathbf{X}^t - \mathbf{X}^*) + (1 - \eta)P_\Omega(\mathbf{X}^t - \mathbf{X}^*)\|_F \\
&\quad + |1 - \eta|\|P_\Omega(\mathbf{X}^t - \mathbf{X}^*)\|_F, \tag{23}
\end{aligned}$$

where (a) is using the Mankowski inequality, (b) follows from

$$\|\mathbf{X}^{t+1} - \mathbf{Z}^{t+1}\|_F = \|P_\Omega(\mathbf{X}^{t+1} - \mathbf{Z}^{t+1}) + P_\Omega^\perp(\mathbf{X}^{t+1} - \mathbf{Z}^{t+1})\|_F,$$

and (c) is according to the Eckart-Young-Mirsky theorem.

Now assume that the sampling density  $p$ , the dimension of  $\mathbf{X}$  and the sparsity level of  $\mathbf{X}$  are given. We establish a relation between  $\|P_\Omega^\perp(\mathbf{X}^t - \mathbf{X}^*) + (1 - \eta)P_\Omega(\mathbf{X}^t - \mathbf{X}^*)\|_F$  and  $|1 - \eta|\|P_\Omega(\mathbf{X}^t - \mathbf{X}^*)\|_F$  via assuming a function  $M(\eta)$  that

$$\begin{aligned}
&\|P_\Omega^\perp(\mathbf{X}^t - \mathbf{X}^*) + (1 - \eta)P_\Omega(\mathbf{X}^t - \mathbf{X}^*)\|_F \\
&= M(\eta)|1 - \eta|\|P_\Omega(\mathbf{X}^t - \mathbf{X}^*)\|_F, \tag{24}
\end{aligned}$$

with  $0 < M(\eta) < 1 + c_1(1 - p)/(c_2p|1 - \eta|)$ , where  $c_1$  and  $c_2$  are constants that satisfy

$$\begin{aligned}
\|P_\Omega^\perp(\mathbf{X}^t - \mathbf{X}^*)\|_F &= c_1(1 - p)\|\mathbf{X}^t - \mathbf{X}^*\|_F \\
\|P_\Omega(\mathbf{X}^t - \mathbf{X}^*)\|_F &= c_2p\|\mathbf{X}^t - \mathbf{X}^*\|_F. \tag{25}
\end{aligned}$$

Hence

$$\|P_\Omega^\perp(\mathbf{X}^t - \mathbf{X}^*)\|_F = \frac{c_1(1 - p)}{c_2p} \|P_\Omega(\mathbf{X}^t - \mathbf{X}^*)\|_F.$$

Due to

$$\begin{aligned}
&\|P_\Omega^\perp(\mathbf{X}^t - \mathbf{X}^*) + (1 - \eta)P_\Omega(\mathbf{X}^t - \mathbf{X}^*)\|_F \\
&\leq \|P_\Omega^\perp(\mathbf{X}^t - \mathbf{X}^*)\|_F + |1 - \eta|\|P_\Omega(\mathbf{X}^t - \mathbf{X}^*)\|_F \\
&= \left(\frac{c_1(1 - p)}{c_2p|1 - \eta|} + 1\right)|1 - \eta|\|P_\Omega(\mathbf{X}^t - \mathbf{X}^*)\|_F,
\end{aligned}$$

we have

$$M(\eta) \leq 1 + \frac{c_1(1 - p)}{c_2p|1 - \eta|}.$$

Then rewrite (23) by using the relation in (24), we have

$$\begin{aligned}
\sqrt{2\psi(\mathbf{X}^{t+1})} &\leq (M(\eta) + 1)|1 - \eta|\|P_\Omega(\mathbf{X}^t - \mathbf{X}^*)\|_F \\
&= (M(\eta) + 1)|1 - \eta|\sqrt{2\psi(\mathbf{X}^t)}. \tag{26}
\end{aligned}$$

In order to guarantee the convergence, we have  $(M(\eta) + 1)|1 - \eta| \leq 1$ . Hence we can choose  $\eta$  as

$$1 - 1/(M(\eta) + 1) < \eta < 1 + 1/(M(\eta) + 1), \tag{27}$$

where  $1 + 1/(M(\eta) + 1) > 1$ . This analysis suggests that it is possible to choose  $\eta > 1$ .

## REFERENCES

- [1] L. Wei, R. Hu, Y. Qian, and G. Wu, "Key elements to enable millimeter wave communications for 5G wireless systems," *IEEE Wireless Commun.*, vol. 8, No. 5, pp. 831–846, Oct. 2014.
- [2] A. Alkhateeb, O. El Ayach, G. Leus, and R. W. Heath, "Channel estimation and hybrid precoding for millimeter wave cellular systems," *IEEE J. Sel. Topics Signal Process.*, vol. 8, No. 5, pp. 831–846, Oct. 2014.
- [3] R. Méndez-Rial, C. Rusu, A. Alkhateeb, N. Gonzlez-Prelcic, and R. W. Heath, "Channel estimation and hybrid combining for mmWave: Phase shifters or switches?" *IEEE Access*, May 2016
- [4] T. S. Rappaport, G. R. MacCartney, M. K. Samimi, and S. Sun "Wideband millimeter-wave propagation measurements and channel models for future wireless communication system design," *IEEE Trans. Commun.*, vol. 63, No. 9, pp. 3019–3056, Sept. 2015.
- [5] J. Lee, G. T. Gil, and Y. H. Lee, "Exploiting spatial sparsity for estimating channels of hybrid MIMO systems in millimeter wave communications," *Proc. 2014 IEEE Globecom*.
- [6] A. B. Smolders, A. C. F. Reniers, U. Johannsen, and M. H. A. J. Herben, "Measurement and calibration challenges of microwave and millimeter-wave phased-arrays," *In 2013 International Workshop on Antenna Technology (iWAT)*, 2013 pp. 358–361.
- [7] W. Tian, P. Huang, K. Han, Q. Liu and X. Peng, "Array error calibration methods in downward-looking linear-array three-dimensional synthetic aperture radar," *J Appl Remote Sens.*, vol. 10, no. 2, pp. (025010)1–20, May 2016.
- [8] T. Djerafi, N. Ghassemi, O. Kramer, O. Youzkatli-EI-Khatib, A. B. Guntupalli and K. Wu, "Small footprint multilayered millimeter-wave antennas and feeding networks for multi-dimensional scanning and high-density integrated systems," *Radioengineering*, vol. 21, no. 4, pp. 935–945, Dec. 2012.
- [9] S. J. Park, D. H. Shin and S. O. Park, "Low side-lobe substrate-integrated-waveguide antenna array using broadband unequal feeding network for millimeter-wave handset device," *IEEE Trans. Antennas Propag.*, vol. 64, no. 3, pp. 923–932, Mar. 2016.
- [10] L. Yang and K. C. Ho, "Alleviating sensor position error in source localization using calibration emitters at inaccurate locations," *IEEE Trans. Signal Process.*, vol. 58, no. 1, pp. 67–83, Jan. 2010.
- [11] B. Liao, J. Wen, L. Huang, C. Guo and S.C. Chan, "Direction Finding With Partly Calibrated Uniform Linear Arrays in Nonuniform Noise," *IEEE Sensors J.*, vol. 16, no. 12, pp. 4882–4890, June 2016.
- [12] E. J. Candès, Y. Eldar, D. Needell, and P. Randall, "Compressed sensing with coherent and redundant dictionaries," *Appl. Comput. Harmonic Anal.*, vol. 31, no. 1, pp. 59–73, July 2011.
- [13] Y. Chi, L. L. Scharf, A. Pezeshki, and A. R. Calderbank "Sensitivity to basis mismatch in compressed sensing," *IEEE Trans. Signal Process.*, vol. 59, no. 5, pp. 2182–2195, May 2011.
- [14] E. J. Candès and T. Tao, "The power of convex relaxation: Near-optimal matrix completion," *IEEE Trans. Inf. Theory*, vol. 56, no. 5, pp. 2053–8080, May 2010.
- [15] R. Meka, P. Jain, and I. S. Dhillon, "Guaranteed rank minimization via singular value projection," *Neural Inf. Process. Syst.*, pp. 937–954, 2010.
- [16] W. U. Bajwa, J. Haupt, A. M. Sayeed, and R. Nowak, "Compressed channel sensing: A new approach to estimating sparse multipath channels," *Proc. IEEE*, vol. 98, no. 6, pp. 1058–1076, May 2010.
- [17] A. M. Sayeed, "Deconstructing multiantenna fading channels," *IEEE Trans. Signal Process.*, vol. 50, no. 10, pp. 2563–2579, Oct. 2002.
- [18] J. Lee, G. T. Gil, and Y. H. Lee, "Channel estimation via orthogonal matching pursuit for hybrid MIMO systems in millimeter wave communications," *IEEE Trans. Commun.*, vol. 64, no. 6, pp. 2370–2386, Apr. 2016.
- [19] J.-F. Cai, E. Candès, and Z. Shen, "A singular value thresholding algorithm for matrix completion," *SIAM J. Optim.*, vol. 20, no. 4, pp. 1956–1982, Mar. 2010.
- [20] Z. Wang and X. Wang, "Low-rank matrix completion for array signal processing," *Proc. 2012 ICASSP*.
- [21] E. J. Candès and Y. Plan, "Matrix completion with noise," *Proc. IEEE*, vol. 98, no. 6, pp. 925–936, May 2010.
- [22] O. E. Ayach, R. W. Heath, S. Abu-Surra, S. Rajagopal, and Z. Pi, "The capacity optimality of beam steering in large millimeter wave MIMO systems," *Proc. 2012 SPAWC Workshop*.
- [23] W. Shen, L. Dai, B. Shim, S. Mumtaz, and Z. Wang, "Joint CSIT acquisition based on low-rank matrix completion for FDD massive MIMO systems," *IEEE Commun. Lett.*, vol. 19, no. 12, pp. 2178–2181, Dec. 2015.
- [24] M. Akdeniz, Y. Liu, M. Samimi, S. Sun, S. Rangan, T. Rappaport, and E. Erkip, "Millimeter wave channel modeling and cellular capacity evaluation," *IEEE J. Sel. Areas Commun.*, vol. 32, no. 6, pp. 1164–1179, June 2014.